Proceedings of CHT-17
ICHMT International Symposium on Advances in Computational Heat Transfer

May 28-June 1, 2017, Napoli, Italy

CHT-17-96

A NUMERICAL CODE FOR THE SIMULATION OF NATURAL-CONVECTION COOLING OF SUBSEA ELECTRICAL POWER CONVERTERS

Thomas B. Gradinger[*,§] and Tor Laneryd[**]

[*]ABB Switzerland Ltd., Corporate Research, Baden-Dättwil, Switzerland

[**]ABB Sweden Ltd., Corporate Research, Västerås, Sweden

[§]Correspondence author. Fax: +41 58 586 40 06 Email: thomas.gradinger@ch.abb.com

ABSTRACT Subsea factories are expected to play an important role in future oil production. Cooling of the necessary power converters in a deep-sea environment as a great challenge. Because of their high reliability, passive cooling systems are preferred that rely on natural convection of the oil within the converter tank, and the sea water around it. In the paper, we present a numerical code for 1-d network models of natural-convection cooling specifically developed for subsea converters. Network elements are provided to model converter components such as semiconductor modules mounted on oil-cooled heat sinks. For spatial discretization, the finite-volume method is used, the resulting set of nonlinear equations are solved in Matlab. Measurements of natural-convection cooling of diode heat sink immersed in an oil-filled tub are presented and a 1-d network model is set up to simulate this case. The numerical convergence is verified and temperatures are compared. The comparison yields a first experimental confirmation of the model. Further experiments will be needed to gain experience with the model and refine it where necessary.

INTRODUCTION

To efficiently extract oil and gas, subsea installations are becoming increasingly important. Compared to topside installations, benefits are most significant in deep water, in locations far offshore, and in harsh environment. With recent advances in power and automation technology, it is finally becoming feasible to build an entire *subsea factory* [2013] on the seabed, including power transformers, variable speed drives (VSDs) and switchgear [2016a] as shown in Figure 1. The VSDs are electrical power converters that are used to drive equipment such as pumps and compressors. In depths up to 3'000 m, servicing of equipment is very restricted and reliability is of utmost importance. Efficient and reliable cooling is therefore key in the design of a subsea converter. Power converters installed on land are typically cooled by forced convection of air or water. In a high-pressure environment it is preferable to submerge the converter in an incompressible liquid rather than build an enclosure to withstand the ambient pressure. Particularly suitable is a dielectric liquid such as the mineral oil that is used for power transformers because of its electrical insulation properties. The converter comprises hence an oil-filled tank and, for the cooling of semiconductors and passive components, relies on natural convection. On the left of Figure 2, the basic principle is illustrated by means of a simplified example. The use of a passive cooling system allows to omit a mechanical pump and eliminates its risk of failure.

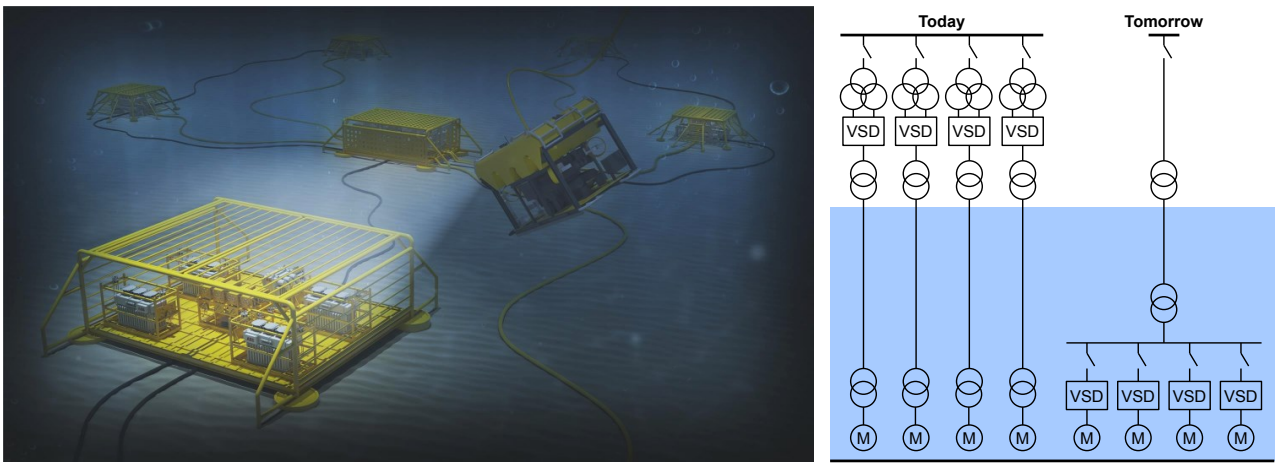

Figure 1. Left: Subsea factory. Right: Subsea power distribution.

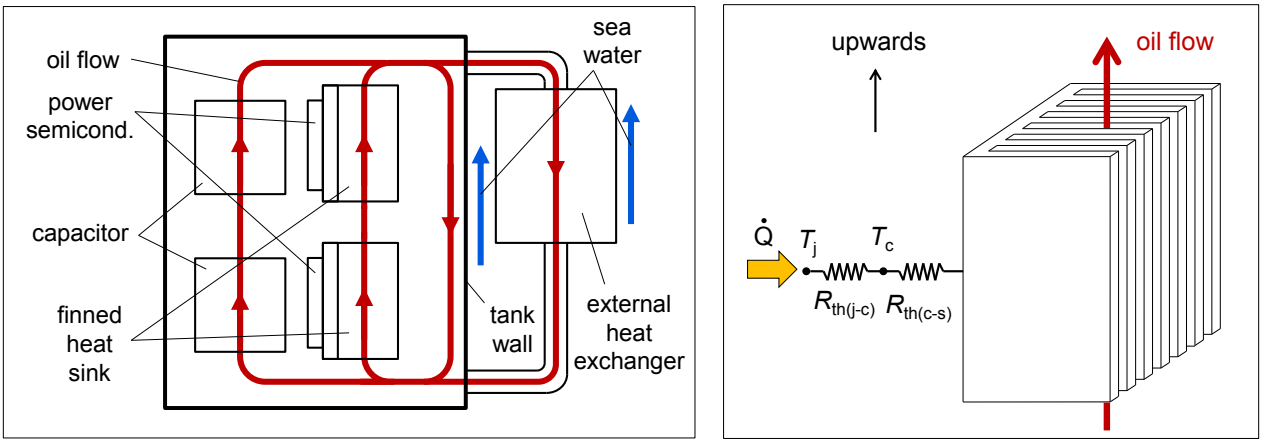

Figure 2. Left: Principle of subsea-converter cooling. Right: Oil flow through heat sink.

Natural convection oil cooling is an area that has been investigated extensively in the context of power transformers. Recommendations for power-transformer thermal design are provided in the loading guides published by the IEEE and IEC standards committees [1999, 2005]. A detailed summary of the state of the art including both thermal network modeling and CFD (computational fluid dynamics) is given in the Technical Brochure by Cigré [2016b]. An instructive example of thermal network modeling for power transformers is available in Del Vecchio et al. [2010]. The published models are developed solely for transformer geometries, and are not applicable for the considerably different geometry of a subsea drive.

MODELING APPROACH

For design and optimization of general cooling systems, different levels of numerical modeling are available. 3-d CFD models are valuable for detailed analysis of specific features of flow and heat transfer. To keep CFD analyses affordable, they must usually be limited to small regions within the overall system, and/or a high degree of symmetry must be assumed. Even then CFD is not suited for quick parameter variation in the frame of a design and optimization phase of the cooling system. An additional challenge is constituted by the convergence difficulties often encountered in the simulation of natural convection.

At the other end of the complexity scale are zero-dimensional models that use a single “plenum” oil temperature within the tank. Such models are not intrinsically capable to predict the vertical temperature gradient within the tank. This means that when a temperature gradient is introduced in a

zero-dimensional model, the system of equations is not closed any more, and additional assumptions must be made. These assumptions are based on measurements and are specific for a certain type of geometry.

In contrast, one-dimensional network models of flow and heat transfer naturally provide a spatial resolution of temperature. In particular, with vertically oriented elements, the vertical temperature stratification in the tank is obtained. Being much faster than CFD models, 1-d models are well suited for cooling-system dimensioning, fast parameter variation, and even automatic optimization.

We will consider a numerical model appropriate for the design of the passive cooling system of a subsea converter. The thermal chain from loss-generating components to the ambient sea water involves natural convection first in the oil, from the components to the tank wall; and second in the sea water, from the tank wall to the ambient. The primary focus will be on the oil-side heat transfer, where a 1-d model is required to predict the temperature gradients that drive oil circulation. On the sea-water side, a zero-dimensional model is considered sufficient.

LABORATORY TEST

As an application case for the simulation code, we use a laboratory test in an oil tub. We introduce the test setup here, because later on, we will refer to it when describing the network model in more detail. Two diode modules, designed for subsea use, were clamped between finned aluminum heat sinks and immersed in a steel tub as shown in Figure 3. The tub was filled with mineral oil of the type Nytro 10XN. The oil rises through the diode heat sinks to the free surface and returns through a finned water-cooled heat sink. The geometry of the laboratory test is relevant for the oil circulation, but is not representative of the sea-water cooling of the converter tank walls. The tub was placed in an air-filled room. A small portion of the heat is transferred to the ambient air via the tank wall and natural convection in the air. In addition to the diode there is further energy input into the oil due to losses in bus bars and connections. The different fin lengths of the heat sinks shown in Figure 3 on the right are due to the fact that each diode has a collector and an emitter side, where the majority of the losses is transferred to the collector side.

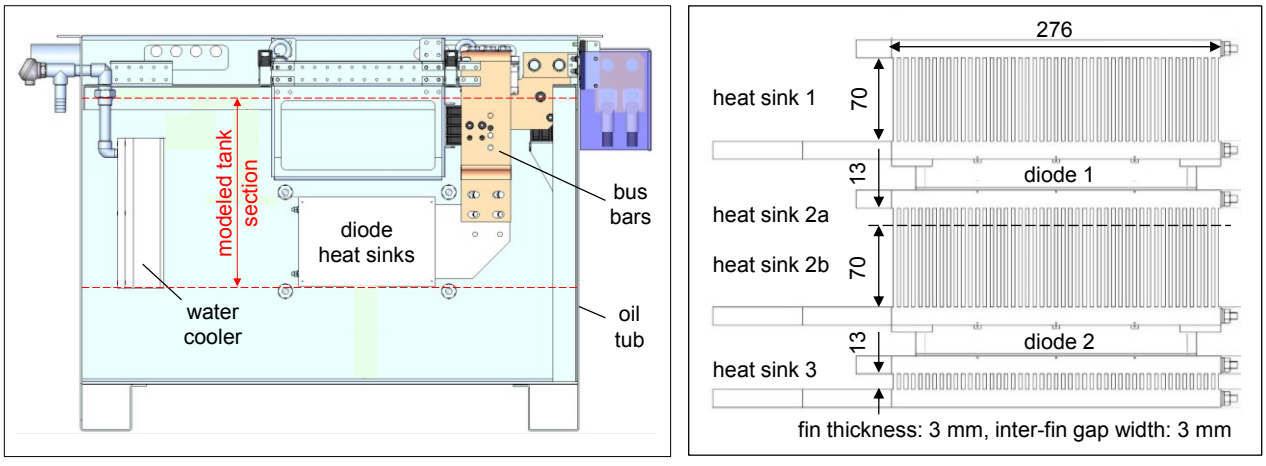

Figure 3. Cooling test in oil tub. Left: Side view of tub. Right: Top view of semiconductor modules and heat sinks.

NETWORK MODEL

The 1-d oil-flow network model can be represented by a graph that consists of nodes and elements connecting the nodes, where the elements correspond to the channels or flow pathways. In Figure 4

the network of the laboratory test is shown as an example. The modeling of an entire subsea converter is done in a similar way. Thermally, every node is assumed to act as a perfect mixer. This means the node temperature results – according to energy conservation – from the inflowing oil streams of the node; while each outflowing oil stream has the node temperature. Mass and energy conservation is enforced for the nodes, while momentum conservation is enforced for every independent loop in the network, and energy conservation is enforced along the elements.

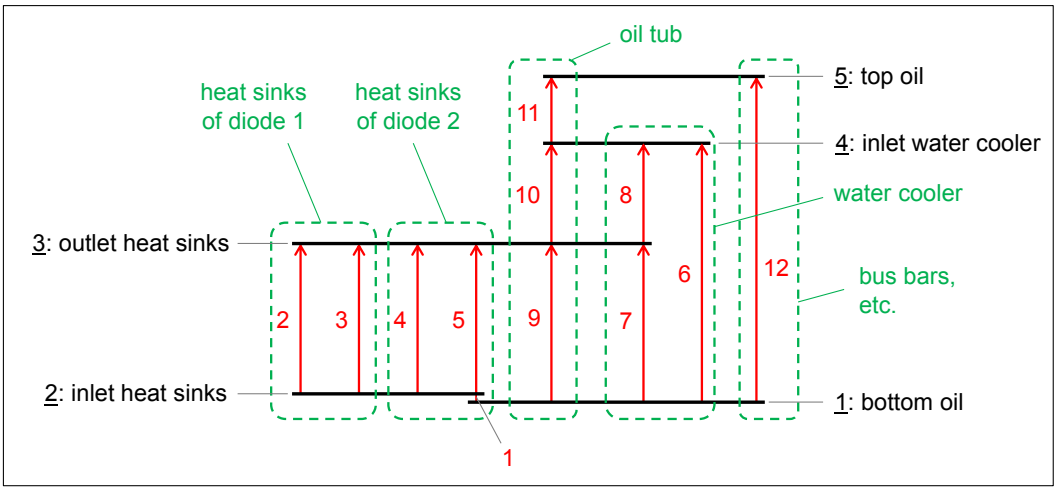

Figure 4. Flow network of test in oil tub. Horizontal lines = nodes, vertical lines = elements. Node numbers underlined. Element types: 1 = adiabatic channel, 2 to 5 = semiconductor heat sink, 6 = external heat exchanger, 7 to 11 = tank, 12 = heated channel. Arrows indicate in which direction $\dot{m}$ is defined to be positive.

For the pressure p as a function of the vertical coordinate z along a channel, we get, from conservation of momentum,

$$\frac{\mathrm{d}p}{\mathrm{d}z} = \left(\rho_0 - \rho(\bar{T}_V)\right)g - \frac{P}{A}\tau_\mathrm{w} \tag{1}$$

Here, ρ_0 is a reference density, g gravitational acceleration, P channel perimeter, A channel cross-section and τ_w wall shear stress. $\bar{T}_V$ is the volumetric temperature mean over a channel cross-section. Conservation of energy in an element reads

$$\dot{m}\frac{\mathrm{d}}{\mathrm{d}z}\left(c_p\bar{T}\right) = \dot{Q}' \tag{2}$$

where $\bar{T}$ is the velocity-weighted temperature mean over the channel cross-section, c_p is specific heat at constant pressure, $\dot{Q}'$ is the external heat-flow rate per channel length into the channel, and $\dot{m}$ is the mass-flow rate in the channel. From Eqs. (1) and (2), we see that we need both $\bar{T}(z)$ and $\bar{T}_V(z)$. Since, from the energy equation, we only get $\bar{T}(z)$, we need a relation between $\bar{T}(z)$ and $\bar{T}_V(z)$. This is expressed by

$$\gamma \equiv \frac{\bar{T}_V - T_\mathrm{w}}{\bar{T} - T_\mathrm{w}} \tag{3}$$

where $T_\mathrm{w}(z)$ is the local wall temperature. Next to γ, for any channel element, we need a correlation for the Nusselt number Nu to express $\dot{Q}'$, and for the friction coefficient ζ_f to express τ_w.

ELEMENT TYPES

In our 1-d network code, several element types are predefined. They are introduced in the following, and it is explained how they are used to model the laboratory test.

Semiconductor Heat Sink This element type is based on parallel connected rectangular vertical ducts, representing the flow in the inter-fin gaps as shown in Figure 2 on the right. The correlations for Nu, ζ_f, and γ take into account the thermal entrance effect and the influence of local buoyancy. They were derived from 2-d CFD simulations of laminar flow between vertical parallel plates. The correction factors that multiply the forced-flow limits of Nu, τ_w and γ are of the form

$$F_i = 1 + A_i f_i^{B_i} \tag{4}$$

where

$$f_i = \frac{\mathrm{Gr}_{2s,\mathrm{loc}}}{\mathrm{Re}_{2s}} \left(1 - a_i e^{-z^*/b_i}\right) \tag{5}$$

Here, i stands for either Nu, τ or γ. Gr is a local Grashof number based on

$$\Delta T_{\mathrm{w\text{-}c}}(z) \equiv T_w(z) - \bar{T}(z) \tag{6}$$

and the index "$2s$" means reference to twice the channel width s as a length scale. The nondimensional distance to the channel inlet is defined as

$$z^* \equiv z/z_{\mathrm{ref}} \tag{7}$$

where

$$z_{\mathrm{ref}} \equiv 3\bar{v}s^2/(8\alpha) \tag{8}$$

$\bar{v}$ is the mean velocity of forced flow in the channel cross-section, and α is the thermal diffusivity. The constants are: $A_{\mathrm{Nu}} = 4 \cdot 10^{-4}$, $A_\tau = 2.35 \cdot 10^{-3}$, $A_\gamma = 3.8 \cdot 10^{-4}$, $B_{\mathrm{Nu}} = B_\tau = 1.1$, $B_\gamma = 1$ $a_{\mathrm{Nu}} = 0.8$, $a_\tau = 0.6$, $a_\gamma = 0.95$, $b_{\mathrm{Nu}} = b_\tau = b_\gamma = 0.07$. For the forced-flow limit of Nu, see e.g. Rohsenov et al. [1998]. For the forced-flow limit of τ_w, developed laminar flow is assumed, which is a fair assumption on account of the high Prandtl number of oil and the rapid hydraulic development of the flow. A separate publication is planned on the derivation of corrections (4).

The *semiconductor heat sink* element model comprises further the fin equations (see e.g. Incropera et al. [2007]) and the thermal resistance of the heat-sink base plate. Like the oil flow, the heat-sink temperature depends on the vertical coordinate z. Heat conduction in the heat sink in z-direction is currently not considered. This simplification has the advantage of retaining the parabolic nature of the equations, an aspect that will be discussed further below. A more detailed model including full heat spreading within the heat sink is subject to a future model extension. Based on the heat-sink base-plate temperature, the junction temperature of a mounted semiconductor module is calculated from an additional thermal resistance $R_{\mathrm{th(j\text{-}c)}}$ (junction to module case) and $R_{\mathrm{th(c\text{-}s)}}$ (module case to heat sink).

In the network of the oil-tub test, elements 2 to 5 are of the type *semiconductor heat sink*, representing heat sink 1, 2a, 2b, and 3 shown in Figure 3 on the right. Heat sinks 2a and 2b correspond to a virtual division of heat sink 2, with fin lengths proportional to the losses transferred in their direction. This allows the use of the same element type for all the heat sinks.

Heated Channel This element type represents a number of parallel-connected rectangular vertical channels with pre-defined heat input. It can be used to model passive components such as ducted transformer windings or capacitors. The oil-flow model is similar as in the semiconductor heat sink. In the network of the oil-tub test, element 12 is of type *heated channels* and is used to represent the heat input via bus bars.

Adiabatic Channel This element type is used for wide sections of vertical flow without heat transfer, and with negligible wall friction forces. Only the buoyancy contributes to the momentum balance. One possible usage is the modeling of vertical gaps between stacked loss-generating components, where the oil flow rises from a lower to the next higher component. If there is a cooled tank wall at the same height, then the *tank* element should be used instead, and it is not necessary to connect an

adiabatic channel in parallel. For the modeling of the oil-tub test, an *adiabatic channel* element is used only to connect nodes 1 and 2, which are very close, to avoid splitting up elements 7 and 9.

Horizontal Flow Resistance In some cases, there may be parallel or antiparallel vertical flow paths with "leakage" between them. This can be modeled by horizontally connecting nodes between the two paths via a flow resistance. It can be defined to depend linearly and/or quadratically on the flow rate. For the modeling of the oil-tub test, this element type is not necessary.

External Heat Exchanger An external, sea-water cooled heat exchanger is represented by a number of parallel vertical channels, separated from the ambient sea water by a conducting wall. Optionally, there can be fins on the oil side of the wall, in which case the fin efficiency is considered like in the *semiconductor heat sink* element. On the sea-water side, the Nu correlation by Churchill and Chu [1975] for natural-convection heat transfer at a vertical wall in a plenum is used. In the network of the oil-tub test, element 6 is of type *external heat exchanger* and is used to represent the fin part of the water cooler.

Tank This element type is needed to represent cooling on the inside of the converter tank, with a downward flowing boundary layer of oil adjacent to plenum oil as shown in Figure 5 on the left. The same Nu correlation for natural convection at a vertical wall is used as in the *external heat exchanger* element. The mass-flow rate in the element at any vertical position is the sum of the mass-flow rate $\dot{m}_{\mathrm{BL}}$ and $\dot{m}_{\mathrm{pl}}$ in the boundary layer and plenum oil, respectively. Compared to the boundary layer, the plenum oil is almost stagnant. However, since its flow cross-section is large, even very low plenum velocities can result in non-negligible mass-flow rates. We therefore set the frictional pressure drop of the tank element to zero, independent of mass-flow rate. This property is shared with the *adiabatic channel* element.

To determine the heat-transfer coefficient for natural convection at the wall, the volumetric mean plenum oil temperature is needed. (This reflects, as mentioned above, the need to know γ for any element.) Because of the low conductivity of oil and the large extensions of the plenum in the applications of interest to us, convection dominates the temperature distribution in the plenum. As can be seen Figure 5 on the left, mass conservation requires that

$$\dot{m} = \dot{m}_{\mathrm{pl,top}} = \dot{m}_{\mathrm{pl,bot}} + \dot{m}_{\mathrm{BL}} \tag{9}$$

In case $\dot{m} \geq \dot{m}_{\mathrm{BL}}$, there is a downward velocity in the entire plenum, since the boundary layer is fed from above. It is then reasonable to assume that $\bar{T}_{\mathrm{V}} = T_{\mathrm{n,top}}$, where $T_{\mathrm{n,top}}$ is the top node temperature of the element. Conversely, if $\dot{m} = 0$, all fluid feeding the boundary layer must come from below, such that $\bar{T}_{\mathrm{V}} = T_{\mathrm{n,bot}}$. For $\dot{m}$ between 0 and $\dot{m}_{\mathrm{BL}}$, a simple approach is to linearly interpolate, as shown in Figure 5 on the right. This requires, however, knowledge of $\dot{m}_{\mathrm{BL}}$, a quantity which is normally not given by engineering correlations for natural-convection heat transfer (compare e.g. Rohsenow et al. [1998]). We therefore, for the time being, use a fixed weighting factor f_{TV} to calculate $\bar{T}_{\mathrm{V}}$:

$$\bar{T}_{\mathrm{V}} = f_{\mathrm{TV}} T_{\mathrm{n,top}} + \left(1 - f_{\mathrm{TV}}\right) T_{\mathrm{n,bot}} \tag{10}$$

The value chosen for f_{TV} will be discussed in the Results section.

The treatment of the *tank* element in the energy equation is somewhat special. Since $\dot{m}$ may be zero, we cannot use Eq. (2). Rather, the heat-flow rate $\dot{Q}$ transferred to the ambient through the tank wall must be directly extracted from the bottom node of the *tank* element. This is physically reasonable as the cold boundary-layer oil flows down into the bottom node, see Figure 5.

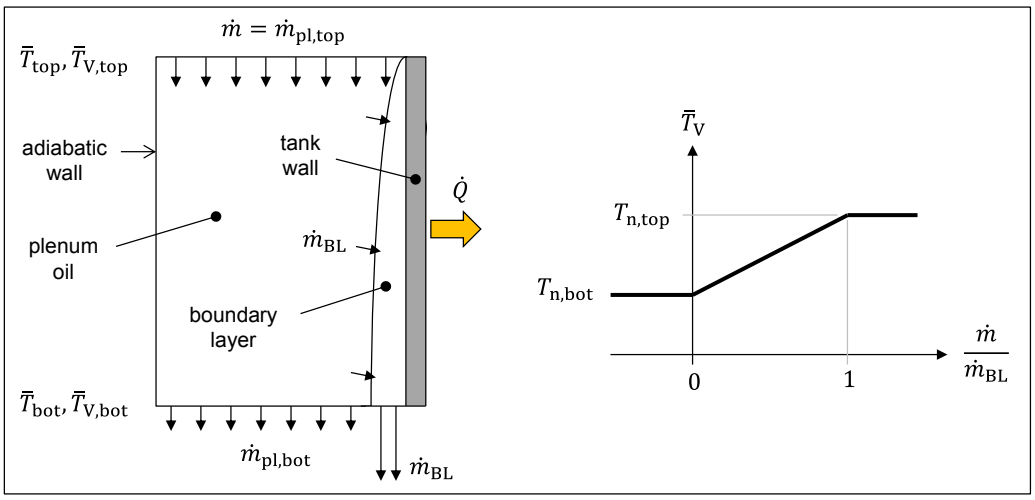

Figure 5. Left: Tank element. Right: Model for $\bar{T}_{\mathrm{V}}$ of the tank element.

In the oil-tub network, the *tank* element is used to represent both the flat back side of the water cooler and the tub. Elements 7 and 8, representing the water cooler, have water as ambient fluid, with an external heat-transfer coefficient representing forced convection. Elements 9 to 11, representing the tub, have air as ambient fluid, with the external heat-transfer coefficient calculated for natural convection. In the tests, a persistent oil-temperature stratification was observed in the tub, meaning that the oil below the heat sinks stayed cold. As a result, the lower part of the oil tub did not participate in the heat transfer to air. Consequently, the network model only extends to the bottom of the heat sinks. The tub section included in the network model is indicated in Figure 3 on the left.

The water-cooler back side is split into elements 7 and 8 to enable connection with node 3 and enforce a uniform pressure at the height of this node. For the same reason, the tub is represented by three *tank* elements in series: elements 9, 10, and 11. This enables connection with nodes 3 and 4. When using multiple series-connected *tank* elements to represent a single real wall, we base the Nu correlations on the real wall height, i.e. on the sum of the heights of the series-connected *tank* elements. This makes sense as the boundary layer is not interrupted at the connecting nodes. For the same reason, the heat-flow rate $\dot{Q}$ transferred to the ambient by all series-connected *tank* elements is subtracted from the *bottom* node of the *lowest* tank element.

Tank elements can be connected in parallel as is for example the case with elements 7 and 9 in Figure 4. The momentum equation of the corresponding loop (up along element 7 and down along element 9) becomes singular in this case, as the frictional pressure drop does not depend on the mass-flow rate. Instead of solving the momentum equation, we then arbitrarily set one of the element mass-flow rates to zero. This has no further influence on the results.

SOLUTION METHOD

For the iterative solution of the nonlinear equations governing the two-step natural-convection problem, we seek a vector $\boldsymbol{x}$ of primary unknowns that has minimum length. To this end, using graph theory, we identify a complete set of M independent loops and introduce the corresponding independent mass-flow rates $\dot{m}_{\mathrm{ind},m}$. From the $\dot{m}_{\mathrm{ind},m}$, the mass-flow rates $\dot{m}_n$ of the N elements (where $N \geq M$) can then be obtained, and mass is automatically conserved at the nodes.

To discretize the momentum and energy equations in the elements, we use the finite-volume method. Every element is divided into C cells between inlet and outlet. Integrating the momentum equation around each independent loop yields M equations for the M independent mass-flow rates. For the solution of the energy equation, it is essential to realize that, for given mass-flow rates, the equations are parabolic and can be integrated from inlet node to outlet node of the element. This is done using

a predictor-corrector method. It therefore suffices to introduce the K node temperatures as unknowns rather than the much higher number of cell temperatures. As mentioned, on adding heat conduction along the channels, e.g. in a heat sink, the parabolic nature of the equations is lost. To solve the resulting elliptic equations, further primary unknowns must be introduced, or an additional iteration is necessary. Upon integrating to the element outlet temperatures, the K nodal energy equations can be formulated to solve for the K node temperaures.

In the simplest case, there is only one element transferring heat to the ambient sea water. This element is typically the tank. The heat transferred by the element is then known, and the external natural-convection problem can be solved as a preprocessing step prior to solving for $\boldsymbol{x}$. In the general case of H ($H \geq 1$) elements transferring heat to the sea water, we introduce $H-1$ additional primary variable. These are the fractions $f_{Q,1}, \dots, f_{Q,H-1}$ of total losses transferred by the first $H-1$ elements thermally connected to sea water. They allow the calculation of Nu on the sea-water side, which, in natural convection, depends on the heat-flow rate.

The vector of primary unknowns $\boldsymbol{x}$ is hence defined as:

$$\boldsymbol{x} \equiv \left\{\dot{m}_{\mathrm{i},1}, \dots, \dot{m}_{\mathrm{i},M}, T_{\mathrm{n},1}, \dots, T_{\mathrm{n},K}, f_{Q,1}, \dots, f_{Q,H-1}\right\} \tag{11}$$

and has length $M + K + H - 1$.

The system of equations is solved in Matlab using the built-in function *fsolve*. On account of the strong non-linearity, it is not surprising that a good initial guess is needed to facilitate convergence. For large, complex networks, it may be difficult to come up directly with a sufficiently close initial guess. In this case, we found the following procedure to work well:

1. Start with a simpler network and solve it.
2. Add an element. Adapt its parameters such that heat- and mass-flow rates of the element are small, causing only little change to the rest of the network. Use an initial guess similar to that of the simpler network and solve.
3. Gradually change the parameters of the newly added element to the values of actual interest. Adapt the initial guess along the way to get convergence.
4. Go to step 2, adding another element.

Convergence The convergence of the finite-volume method was checked by varying C, the number of cells per element, from 2 to 64 for the example of the oil-tub network. Only for elements of type *adiabatic channel* and *tank*, C was kept equal to 1, since, according to the physical models, there is nothing to spatially resolve. The solution for $C = 128$ was taken as exact reference. The implemented predictor-corrector method is second-order accurate. The convergence plot in Figure 6 showing normalized errors for element 2, indicates a somewhat slower convergence over most of the studied range of C. For increasing C, the order increases and is not far from 2 for large C. Generally, the discretization error is small already for not very large values of C. Practically, using $C = 8$ or 16 yields discretization errors that are small compared to the uncertainties of the physical models and measurements. To be on the safe side, the results for the comparison with the oil-tub test were obtained for $C = 32$.

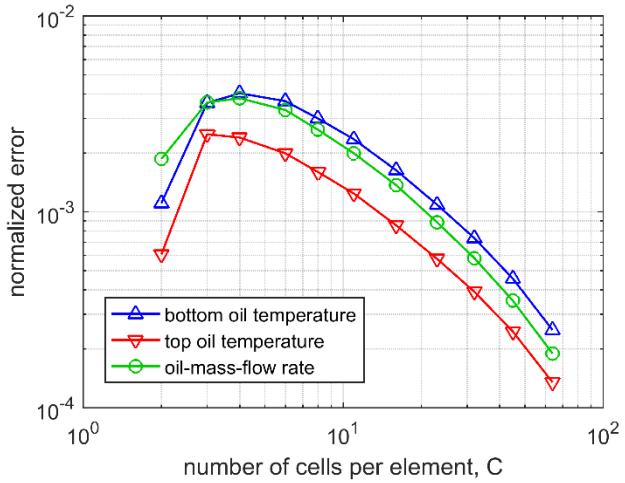

Figure 6. Convergence of mass-flow rate, bottom and top oil temperature of element 2.

RESULTS

A good impression of the simulated results is obtained from a graph of the mean oil temperature in the different elements as a function of the vertical coordinate z as shown in Figure 7. It is seen that the oil flowing through the four diode heat sinks (elements 2 to 5) heats to different outlet temperatures prior to entering node 3. Since, as mentioned, each node acts as a mixer, there is a single outlet temperature into elements 8 and 10. The dashed lines show the downward flowing oil in the water-cooled heat sink and in some of the tank elements. Due to the poor heat transfer on the air side, the tub wall contributes little to the cooling. 97 % of the losses are transferred by the water cooler, with the fins and back side contributing 86 and 14 % to its cooling power, respectively.

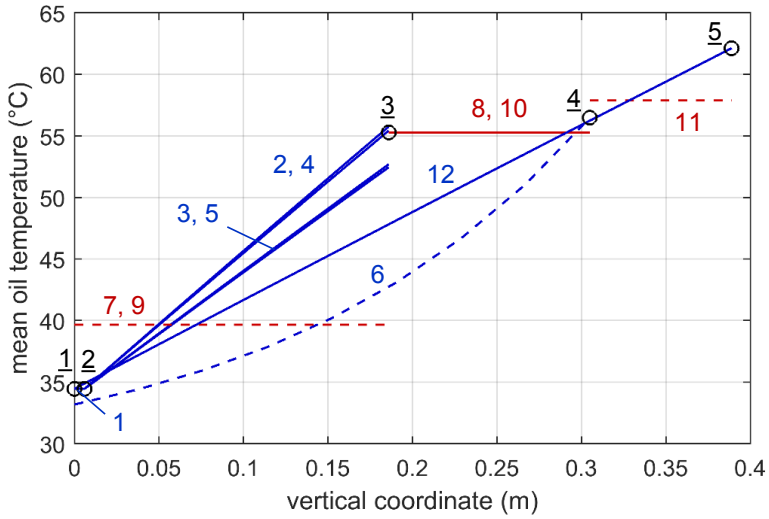

Figure 7. Simulated mean oil temperatures. Node numbers underlined. Solid lines = upward flow, dashed lines = downward flow. Red = tank elements, blue = other elements. $\bar{T}_V$ is shown for tank elements, $\bar{T}$ for all other elements.

In the following, we provide a numerical comparison of temperatures between measurement and simulation. Oil temperatures were measured at inlet and outlet of the diode heat sinks. Temperatures of the heat sinks were measured by thermometers glued to the top and bottom end of the base plates. The water cooler has a rather complex geometry on its water side, making the estimate of the water-side heat-transfer coefficient difficult. In order to avoid inaccuracies due to features that are not the

primary focus of the numerical code, we set the heat-transfer coefficient h_w on the water side to a value of 2'200 $\mathrm{W/(m^2K)}$, which matched the measured bottom oil temperature of 34.3 °C.

For this value, we found good agreement of all top oil temperatures of the IGBT heat sinks when setting the weighting factor f_{TV} of the tank elements to 0.25. As shown in Table 1, the temperatures agree within a few Kelvin, with errors within 10 %. The comparison of the heat-sink temperatures reveals two features. First, the simulated temperatures are more extreme than the measured ones (top too hot, bottom too low). Second, the simulated mean temperature is about 2 to 3 K higher than the measured one. The first phenomenon can clearly be attributed to the non-modeled vertical heat conduction within the heat sink. The second phenomenon is possibly due to a slight underestimation of the base-plate temperatures in the measurements, as the temperature sensors were glued onto the heat sink rather than deeply embedded in holes in the heat sink.

Noticeably, the value of $f_{TV} = 0.25$ found to yield good oil-temperature agreement is lower than 0.5, suggesting that the volumetric mean oil temperature in a tank section is closer to the bottom node than to the top node. In fact, there is a noticeable sensitivity of the results on f_{TV}: For $f_{TV} = 0.5$, the simulated top-oil temperatures of the diode heat sinks are 4 to 5 K higher than the measured ones. We believe that this sensitivity to f_{TV} is a specific feature of the oil-tub setup, where the heat sources and sinks are at almost the same height, resulting in weak buoyancy.

Even though h_w and f_{TV} were *set*, the present comparison serves to support the network model. This is because reasonable agreement was obtained for the oil temperatures with the parameters chosen from a plausible range of values. Clearly, further investigations and experimental comparisons are needed to determine f_{TV} and understand its influence. Refined models for f_{TV} can easily be incorporated into the existing network-modeling framework.

Table 1

Comparison Measurement / Simulation

Diode	Location		T (°C)		ΔT (K)		Error in ΔT	
			Test	Sim.	Test	Sim.	(K)	(%)
bottom oil, plenum			34.3	34.3	–	–	–	–
1	oil	heat sink 1, top	56.5	55.3	22.2	21.0	-1.2	-5
		heat sink 2a, top	54.2	52.3	19.9	18.0	-1.9	-10
	heat-sink base	top, mean	59.6	68.8	25.3	34.5	9.2	36
		bottom, middle	52.3	47.8	18.0	13.5	-4.5	-25
		mean	56.0	58.3	21.7	24.0	2.4	11
2	oil	heat sink 2b, top	56.1	55.6	21.8	21.3	-0.5	-2
		heat sink 3, top	53.9	52.6	19.6	18.3	-1.3	-7
	heat-sink base	top, mean	60.5	69.8	26.2	35.5	9.3	35
		bottom, middle	51.6	48.5	17.3	14.2	-3.1	-18
		mean	56.1	59.2	21.8	24.9	3.1	14

CONCLUSION

Subsea factories are expected to play in important role in future oil production. Cooling of the necessary power converters in a deep-sea environment is a great challenge. Because of their high reliability, passive cooling systems that rely on natural convection of the oil within the converter tank and the sea water around it are preferred .

For the dimensioning and optimization of such systems, 1-d network models are useful tools. They allow quick simulation of global oil flow and temperature distributions. 1-d models are also suited to provide the boundary conditions for 3-d CFD models used to investigate subsystems in more detail.

A 1-d network suited to analyze power converters requires network elements specifically developed for this application. A corresponding numerical code, based on the finite-volume method, has been developed and tested. Because of the strong nonlinearity of the problem, numerical convergence requires a good initial guess. Such a guess can be obtained using a simple algorithm.

One network element that needs special attention is the *tank* element, representing a cooled vertical wall bounded by a plenum of oil. Calculation of the volumetric mean temperature of such an element is key. The 1-d network model was successfully applied to the measured configuration of semiconductor heat sinks immersed in an oil tub. While this is a first confirmation of the model, further comparison with experiments will be needed to gain experience with the model and refine it where necessary.

REFERENCES

Churchill, W. and Chu, H. H. S. [1975], Correlating Equations for Laminar and Turbulent Free Convection from a Vertical Plate, *Int. J. Heat and Mass Transfer*, Vol. 18, pp 1323-1329.

Rohsenow, W. M., Hartnett, J. P., and Cho, Y. I. [1998], *Handbook of Heat Transfer*, 3rd Edition, McGraw-Hill.

IEEE C57.96 [1999], *Guide for loading dry-type, distribution and power transformers*.

IEC 60076-7 [2005], *Power Transformers Part 7: Loading Guide for oil immersed power transformers*.

Incropera, F. P., DeWitt, D. P., Bergmann, T. L, and Lavine, A. S. [2007], *Fundamentals of Heat and Mass Transfer*, 6th ed., John Wiley & Sons.

Del Vecchio, R. M., Poulin, B., Feghali, P. T., Shah, D. M., and Ahuja, R. [2010], *Transformer Design Principles: With Applications to Core-Form Power Transformers*, 2nd Edition, CRC Press.

Ramberg, R. M., Davies, S. R. H., Rognoe, H., and Oekland, O. [2013], Steps to the Subsea Factory, *Offshore Technology Conference Brazil*, 29-31 October, Rio de Janeiro, Brazil.

Bugge, J. Ø., Storm-Johannessen, P., and Pretlove, J. [2016a], "Sea Change Advances in Power and Automation will allow an Entire Oil and Gas Production Facility to be Built on the Seabed", *Offshore Technology Conference Asia*, 22-25 March, Kuala Lumpur, Malaysia.

[2016b] Transformer Thermal Modelling, Working Group A2.38, June 2016, Cigré.